PAPER

Enhancement of laser induced Au nanoparticle formation by femtosecond pulse shaping

Laser Phys. **23** (2013) 076004 (5pp) doi:10.1088/1054-660X/23/7/076004

Enhancement of laser induced Au nanoparticle formation by femtosecond pulse shaping

P H D Ferreira[1], D L Silva[2], J P Siqueira[1], D T Balogh[1], S Canuto[2], L Misoguti[1] and C R Mendonca[1]

[1] Instituto de Física de São Carlos, Universidade de São Paulo, Caixa Postal 369, 13560-970 São Carlos, SP, Brazil
[2] Instituto de Física, Universidade de São Paulo, Caixa Postal 66318, 05314-970 São Paulo, SP, Brazil

E-mail: crmendon@if.sc.usp.br

Received 6 December 2012, in final form 4 January 2013
Accepted for publication 8 May 2013
Published 6 June 2013
Online at stacks.iop.org/LP/23/076004

Abstract
We report the control of Au nanoparticle (NP) formation by using shaped 30 fs pulses, in a solution containing $HAuCl_4$ and chitosan. By using a sinusoidal spectral phase, a periodic train of pulses is generated. When the period of the pulse train matches certain Raman resonances of chitosan, the reducing agent of the process, an enhancement of the Au NP formation is observed. Theoretical quantum chemical calculations indicate that the outer groups of the chitosan are mostly influenced by low Raman frequencies, which is in reasonably agreement with the experimental data and indicates an enhancement in the Au NP formation as the pulse train period increases (low frequency).

(Some figures may appear in colour only in the online journal)

1. Introduction

Coherent control of light–matter interaction has been extensively studied in the last few years, motivated by its ability to drive a given process to a specific final state [1, 2]. Such control is achieved, for example, by modulating the spectral phase of ultrashort pulses using pulse shaping methods [3, 4], and has been applied to optimize chemical reactions, control vibration dynamics in molecules and multi-photon excitation [2, 5–10]. At the same time, the processing and synthesis of nanostructured materials has received considerable attention because of its potential applications in different fields of science [11, 12]. Distinct methods have been developed to produce metal nanoparticles (NPs). Such methods include chemical, photochemical and thermal approaches, as well as a combination of these, which has allowed considerable control of the size, shape and morphology of NPs [13, 14]. Because of their unique physical and chemical properties, gold NPs have been employed in fundamental research as well as in chemical and biological applications [15].

In this work, we used 30 fs pulses at 800 nm to reduce gold ions and, consequently, to produce NPs in a solution containing $HAuCl_4$ and chitosan [16], which acts as a reducing agent and stabilizer for the NP formation. By applying sinusoidal spectral phase modulation to the pulse (coherent control), we were able to predominantly excite vibrational modes of the chitosan, associated with its peripheral groups, that enhance the NP formation. Theoretical quantum chemical calculations, based on density functional theory (DFT), were carried out to determine chitosan's Raman spectrum and to support the experimental results' interpretation. Therefore, such results open up new possibilities for controlling the synthesis of metal NPs.

2. Experimental setup

The gold NP production was carried out in a sample containing tetrachloroauric acid ($HAuCl_4$) and chitosan.

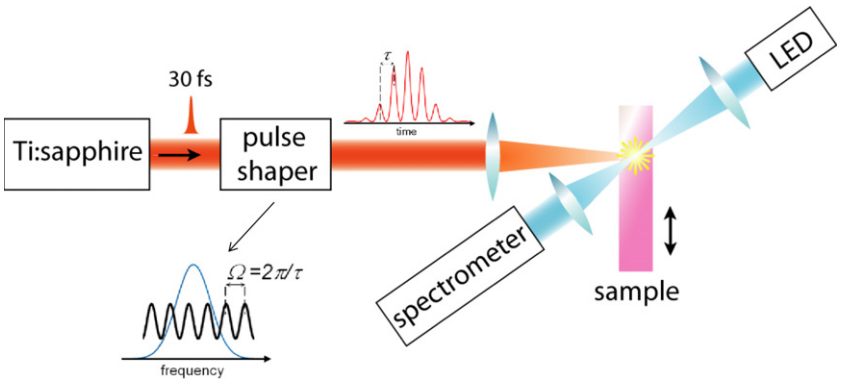

Figure 1. Illustration of the experimental setup used to induce the NP formation and measure the corresponding plasmon band. The angle between both beams in the real experimental setup was approximately 15°. The double arrow next to the sample indicates its vertical agitation, carried out to homogenize the sample.

While the acid provides the gold ions for the photoreduction, chitosan is used as the stabilizer and reducing agent in the process. Chitosan is a linear cationic polysaccharide obtained by deacetylation of chitin, which is normally found in crustaceans and has applications in several areas, from biology to nanotechnology [17, 18]. An aqueous solution of $HAuCl_4$ (0.2 wt%) is mixed with the chitosan solution in a 1:3 volume ratio at room temperature, which corresponds to an approximately equimolar proportion of chitosan repeating units to Au. The sample was placed in a 2 mm path-length quartz cuvette to perform the experiments.

As the excitation source, we used 30 fs pulses (FTL pulses) centered at 800 nm from a Ti:sapphire amplifier and operating at 1 kHz repetition rate. The gold NPs' production was monitored, during fs-laser irradiation, by measuring the plasmon absorption band with the aid of a white light LED and an optical fiber coupled to a spectrometer [16]. The angle between pump and probe beams was approximately 15°. In order to homogenize the distribution of the produced Au NPs, the sample is agitated (5 Hz) perpendicularly to the pump and probe beams throughout the entire experiment. This experimental setup is illustrated in figure 1. Shaping of the excitation pulse was performed by modulating its spectral phase using a pulse shaper based on a 640-element liquid crystal spatial light modulation (SLM) placed at the Fourier plane of a zero dispersion compressor [3]. In our pulse shaper setup, we used a 30 cm cylindrical mirror and 600 lines mm^{-1} diffraction grating. Before the experiments, the pulse is set to the Fourier transform limited one at the sample position.

The pulse shaping system was calibrated using common-path spectral interferometry [19] and the resulting pulses were characterized using frequency-resolved optical gating (FROG) [20]. The sample was irradiated by the shaped fs-pulses with energy of 100 μJ and a beam spot of 1.6 mm. We used a sinusoidal spectral phase modulation $\varphi(\omega) = \alpha \sin(\omega\tau + \delta)$, where α is the modulation depth, τ is the frequency of modulation and δ is the position of the phase mask relative to the center of the pulse spectrum. Such phase modulation allows us to produce a train of fs-pulses, whose relative amplitudes are controlled by α and separation defined by τ.

3. Results and discussion

Figure 2 shows the time evolution of the plasmon band, related to the production of Au NPs, during irradiation with two distinct trains of fs-pulses (shaped pulses), in which the individual pulses are separated by 130 fs (a) and 340 fs (b). It has already been reported that fs-pulses induce the oxidation of hydroxyl to carbonyl groups in chitosan, leading to the reduction of gold ions and consequent production of NPs [16]. No NP formation was observed without fs-laser irradiation. It is worth noting that the sample, either before or after irradiation, is transparent in the region where the fs-pulse excitation is performed (800 nm). Therefore, the process is driven by multi-photon absorption where induced heat is completely negligible. Additionally, no NPs were produced when only the probe beam was present. The spectra presented in figure 2 were collected at time intervals of 10 min, with the last curve obtained at 150 min. As can be seen in figure 2, the final absorbance level attained for pulse trains of 130 fs (a) is approximately 0.23, while such a value is about 0.3 for a pulse train of 340 fs.

To study the dependence of the gold NP formation as a function of the pulses separation in the pulse train, we used five distinct values of τ in the phase mask applied to the pulse (pulse shaper). In figure 3 we plot the final plasmon band magnitude (at 150 min) as a function of the time separation between pulses in the pulse train. From this figure we observed that the production of the Au NPs is favored when the fs-pulses are separated from 240 to 340 fs. When the pulse separation is in the range of 130–190 fs, the final values of the plasmon absorption are similar to the ones achieved when FTL pulses are used (indicated by the dashed line in figure 3).

It is known that when fs-pulses with duration shorter than molecular vibration periods propagate through a material, Raman active molecular vibration modes can be excited [21, 22]. Such excitation is possible when the laser pulse spectrum is broad enough to cover the energy gap from the initial state to the Raman-excited mode. Thus, in this general picture, all vibrational levels with energy within the pulse bandwidth will be excited. Thanks to the development of

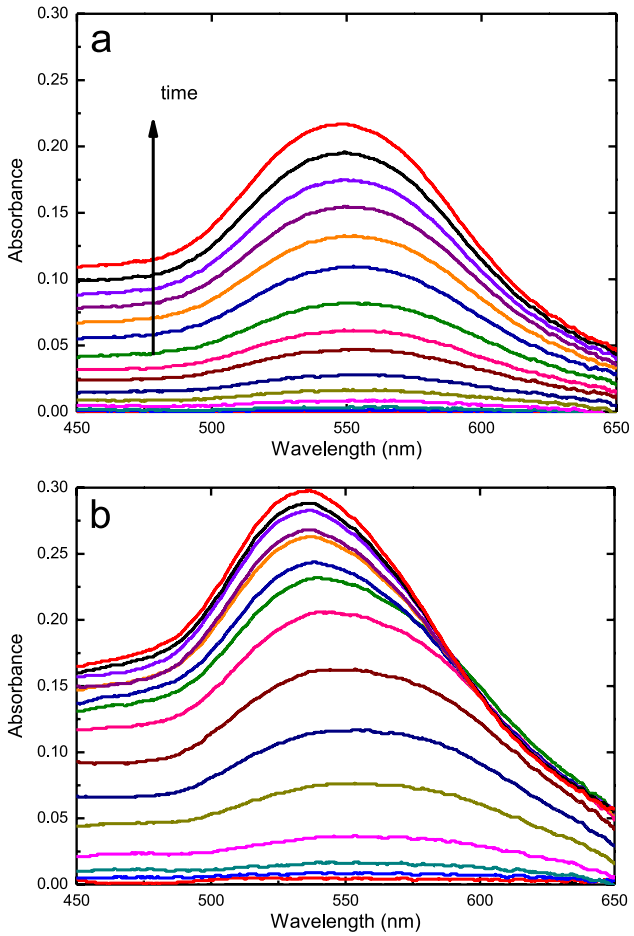

Figure 2. Growth of the surface plasmon absorption band with the irradiation time for pulse trains with a pulse separation time of 130 fs (a) and 340 fs (b). Each curve was obtained at 10 min intervals. The last curve corresponds to 150 min.

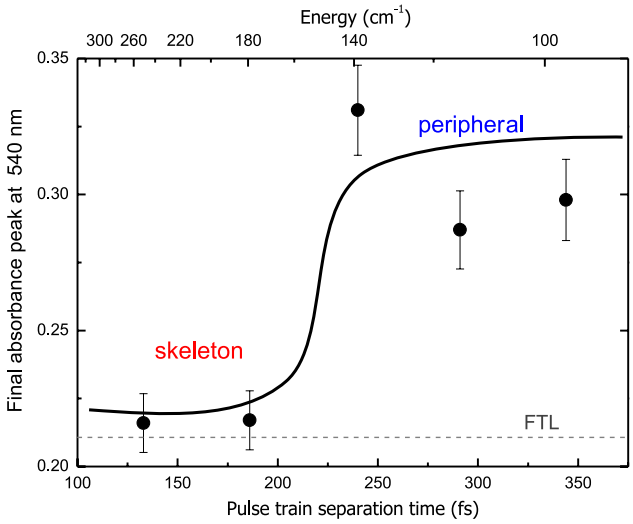

Figure 3. The final plasmon absorption peak as a function of the pulse time separation (bottom axis). The upper axis shows the energy corresponding to the pulse interval. The solid line in this figure is drawn only to guide the eye.

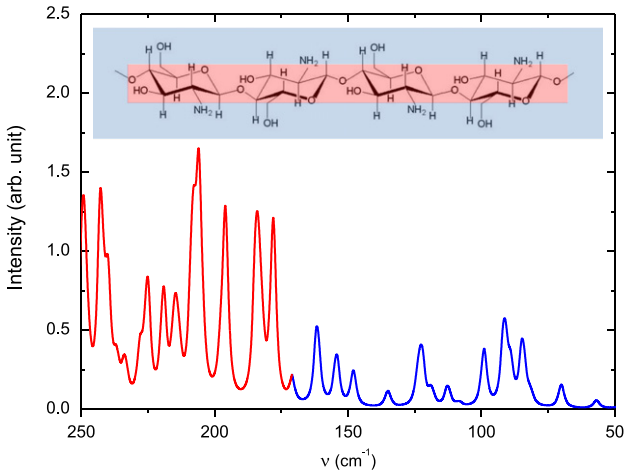

Figure 4. Simulated Raman spectrum of chitosan based on the result of a B3LYP-PCM calculation. The blue line corresponds to the frequency region mainly related to the vibration of the peripheral groups, while the red line illustrates the region mainly associated with the chitosan skeleton movement. The inset shows the molecular structure of a chitosan tetramer, emphasizing peripheral and skeleton groups.

pulse shaping techniques, it has been possible to control the molecular vibrations that are excited. As mentioned before, by applying a sinusoidal spectral phase modulation to the pulse (periodic spectral phase), in the time domain the pulse is split into several equally spaced pulses (pulse trains), whose separation is given by τ. When the vibration mode period is equal to the train time interval (τ), the corresponding vibration mode is effectively excited. In other words, by properly modulating the spectral phase of the pulse, we are able to take advantage of the quantum interference between multiple paths to selectively populate a given vibration level [22, 23].

Therefore, by changing the pulse train period τ, vibrational modes that favor the production of Au NPs could be preferentially excited [22], explaining the result presented in figure 3. To help interpret this result, in the upper axis of figure 3 we show the energy (in cm^{-1}) corresponding to the pulse time separation in the pulse train. As can be seen, for lower energies (below around 150 cm^{-1}) an enhancement of gold NP formation is observed.

In order to verify such a hypothesis, and to understand the observed dependence of the gold NP formation on the pulse train period, we carried out quantum chemical calculations to determine the Raman spectrum of chitosan, since this molecule is the one responsible for the photoreduction of the gold [16, 24]. Quantum chemical calculations were used due to difficulties in obtaining a Raman signal in the energy region of 300–50 cm^{-1}. In the theoretical part of this work, the vibrational activity of chitosan was studied by performing calculations on a chitosan tetramer, illustrated in the inset of figure 4. The equilibrium geometry of chitosan and its Raman vibrational frequencies in the ground state were determined by employing the density functional theory (DFT) method [25, 26]. Also, the polarizable continuum model (PCM) [27–29] was employed to account for the effect of the aqueous environment on the molecular conformation and vibrational activity of chitosan. The geometry optimization

calculation was performed at the B3LYP/6-31G(d) level of approximation [30, 31], while for the Raman vibrational frequency calculation the B3LYP/6-311++G(d,p) level was used. All computations were performed using the Gaussian 03 program package [32]. Over the years, theoretical studies have shown that the combined use of the hybrid B3LYP functional and such basis sets provides reasonable geometries and vibrational frequencies for organic molecules. Harmonic vibrational frequencies were calculated using analytic second derivatives to confirm the convergence to minima on the potential energy surface. At the equilibrium geometry of chitosan no imaginary frequencies were obtained, proving that a global minimum on the potential surface was found. To simulate the Raman spectrum of chitosan in the region of interest, presented in figure 4, the computed frequencies were plotted using a Lorentzian band shape with a bandwidth at the full width at half maximum (FWHM) of 10 cm^{-1}.

The calculated Raman spectrum was analyzed with the aid of the GaussView visualization software. Although the vibrational modes at this low-energy region are not localized, we observed that for the energy region above ∼180 cm^{-1}, vibrations are mainly localized at the skeleton (main chain) of the chitosan structure. However, for energies below approximately 140 cm^{-1}, we observed that torsion motion of peripheral groups, composed mainly of nitrile and hydroxyl, are predominant. Since it has been shown that the reduction of gold ions for the production of NPs is related to the oxidation of hydroxyl groups to carbonyl groups in chitosan [16, 24, 33], it is reasonable to expect that the excitation of vibrational modes of the hydroxyl can improve the NP formation.

4. Conclusions

In this work, 30 fs-pulses at 800 nm are used to produce gold NPs in a solution containing $HAuCl_4$ and chitosan. We demonstrate that fs-pulse shaping, using a sinusoidal spectral phase that generates a periodic train of pulses, can be applied to enhance the synthesis of gold NPs. Our results indicate that the synthesis of gold NPs is favored when the period of the pulse train matches the Raman resonances of the outer groups of chitosan, the reducing agent of the process. Such an interpretation is in agreement with the theoretically calculated Raman spectrum of chitosan, based on the DFT method, which indicates that peripheral groups, which play a major role in the photoreduction process, are more influenced when the pulse train period is increase (low frequency). Thus, pulse shaping methods could be applied to control the synthesis of metal NPs, opening up new possibilities in this area.

Acknowledgments

This work has been supported by Fundação de Amparo à Pesquisa do Estado de São Paulo (FAPESP), Conselho Nacional de Desenvolvimento Científico e Tecnológico (CNPq) and Coordenação de Aperfeiçoamento de Pessoal de Nível Superior (CAPES). We would like to thank Dr Ismael A Heisler for helpful discussions.

References

[1] Warren W S, Rabitz H and Dahleh M 1993 Coherent control of quantum dynamics—the dream is alive *Science* **259** 1581–9
[2] Pastirk I, Brown E J, Zhang Q G and Dantus M 1998 Quantum control of the yield of a chemical reaction *J. Chem. Phys.* **108** 4375–8
[3] Weiner A M 2000 Femtosecond pulse shaping using spatial light modulators *Rev. Sci. Instrum.* **71** 1929–60
[4] Prakelt A *et al* 2003 Compact, robust, and flexible setup for femtosecond pulse shaping *Rev. Sci. Instrum.* **74** 4950–3
[5] Konig K 2000 Multiphoton microscopy in life sciences *J. Microsc.-Oxf.* **200** 83–104
[6] Denk W, Strickler J H and Webb W W 1990 Two-photon laser scanning fluorescence microscopy *Science* **248** 73–6
[7] Rice S A 2001 Interfering for the good of a chemical reaction *Nature* **409** 422–6
[8] Walowicz K A, Pastirk I, Lozovoy V V and Dantus M 2002 Multiphoton intrapulse interference: I. Control of multiphoton processes in condensed phases *J. Phys. Chem.* A **106** 9369–73
[9] Vadim V L, Igor P, Katherine A W and Marcos D 2003 Multiphoton intrapulse interference: II. Control of two- and three-photon laser induced fluorescence with shaped pulses *J. Chem. Phys.* **118** 3187–96
[10] Bordyug N V and Krainov V P 2007 Dynamic resonances in ultra-short laser pulses *Laser Phys. Lett.* **4** 418–20
[11] Cao Y W C, Jin R C and Mirkin C A 2002 Nanoparticles with Raman spectroscopic fingerprints for DNA and RNA detection *Science* **297** 1536–40
[12] Pustovalov V K, Smetannikov A S and Zharov V P 2008 Photothermal and accompanied phenomena of selective nanophotothermolysis with gold nanoparticles and laser pulses *Laser Phys. Lett.* **5** 775–92
[13] Sakamoto M, Fujistuka M and Majima T 2009 Light as a construction tool of metal nanoparticles: synthesis and mechanism *J. Photochem. Photobiol.* C **10** 33–56
[14] Pustovalov V K 2005 Theoretical study of the heating of solid ellipsoidal nanoparticle in media by short laser pulses *Laser Phys. Lett.* **2** 401–6
[15] Daniel M-C and Astruc D 2003 Gold nanoparticles: assembly, supramolecular chemistry, quantum-size-related properties, and applications toward biology, catalysis, and nanotechnology *Chem. Rev.* **104** 293–346
[16] Ferreira P H D *et al* 2012 Femtosecond laser induced synthesis of Au nanoparticles mediated by chitosan *Opt. Express* **20** 518–23
[17] Benavente M 2008 Adsorption of metallic ions onto chitosan: equilibrium and kinetic studies *Thesis* Royal Institute of Technology, Stockholm
[18] Bough WA, Salter W L, Wu A C M and Perkins B E 1978 Influence of manufacturing variables on characteristics and effectiveness of chitosan products: I. Chemical composition, viscosity, and molecular-weight distribution of chitosan products *Biotechnol. Bioeng.* **20** 1931–43
[19] Wilson J W, Schlup P, Lunacek M, Whitley D and Bartels R A 2008 Calibration of liquid crystal ultrafast pulse shaper with common-path spectral interferometry and application to coherent control with a covariance matrix adaptation evolutionary strategy *Rev. Sci. Instrum.* **79** 033103
[20] Trebino R 2000 *Frequency-Resolved Optical Gating: The Measurement of Ultrashort Laser Pulses* (Boston: Kluwer)
[21] Bartels R A, Backus S, Murnane M M and Kapteyn H C 2003 Impulsive stimulated Raman scattering of molecular vibrations using nonlinear pulse shaping *Chem. Phys. Lett.* **374** 326–33
[22] Dudovich N, Oron D and Silberberg Y 2002 Single-pulse coherently controlled nonlinear Raman spectroscopy and microscopy *Nature* **418** 512–4

[23] Mueller C, Buckup T, von Vacano B and Motzkus M 2009 Heterodyne single-beam CARS microscopy *J. Raman Spectrosc.* **40** 809–16
[24] Wei D and Qian W 2008 Facile synthesis of Ag and Au nanoparticles utilizing chitosan as a mediator agent *Colloids Surf.* B **62** 136–42
[25] Hohenberg P and Kohn W 1964 Inhomogeneous electron gas *Phys. Rev.* B **136** B864–71
[26] Kohn W and Sham L J 1965 Self-consistent equations including exchange and correlation effects *Phys. Rev.* **140** A1133–8
[27] Barone V, Cossi M and Tomasi J 1997 A new definition of cavities for the computation of solvation free energies by the polarizable continuum model *J. Chem. Phys.* **107** 3210–21
[28] Mennucci B and Tomasi J 1997 Continuum solvation models: a new approach to the problem of solute's charge distribution and cavity boundaries *J. Chem. Phys.* **106** 5151–8
[29] Miertus S, Scrocco E and Tomasi J 1981 Electrostatic interaction of a solute with a continuum—a direct utilization of ab initio molecular potentials for the prevision of solvent effects *Chem. Phys.* **55** 117–29
[30] Becke A D 1993 Density-functional thermochemistry: III. The role of exact exchange *J. Chem. Phys.* **98** 5648–52
[31] Lee C T, Yang W T and Parr R G 1988 Development of the Colle–Salvetti correlation-energy formula into a functional of the electron-density *Phys. Rev.* B **37** 785–9
[32] Frisch M J *et al* 2003 *GAUSSIAN 03* (Pittsburgh, PA: Gaussian Inc.)
[33] Wei D and Qian W 2006 Chitosan-mediated synthesis of gold nanoparticles by UV photoactivation and their characterization *J. Nanosci. Nanotechnol.* **6** 2508–14